# Metabolomics screening identifies reduced L-carnitine to be associated with progressive emphysema

Thomas M. Conlon\*, Jörg Bartel†, Korbinian Ballweg\*, Stefanie Günter\*, Cornelia Prehn‡, Jan Krumsiek†, Silke Meiners\*, Fabian J. Theis†, Jerzy Adamski‡§||, Oliver Eickelberg\*¶ and Ali Önder Yildirim\*

\*Comprehensive Pneumology Center, Institute of Lung Biology and Disease, Helmholtz Zentrum München, Member of the German Center for Lung Research, Ingolstädter Landstr. 1, 85764 Neuherberg, Germany

†Institute of Computational Biology, Helmholtz Zentrum München, Ingolstädter Landstr. 1, 85764 Neuherberg, Germany

†Institute of Experimental Genetics, Genome Analysis Center, Helmholtz Zentrum München, Ingolstädter Landstr. 1, 85764 Neuherberg, Germany §German Center for Diabetes Research, Helmholtz Zentrum München, Ingolstädter Landstr. 1, 85764 Neuherberg, Germany

||Chair for Experimental Genetics, Technical University of Munich, 85354 Freising-Weihenstephan, Germany

¶Klinikum der Universität München, Max-Lebsche-Platz 31, 81377 München, Germany

#### **Abstract**

Chronic obstructive pulmonary disease (COPD) is characterized by chronic bronchitis, small airway remodelling and emphysema. Emphysema is the destruction of alveolar structures, leading to enlarged airspaces and reduced surface area impairing the ability for gaseous exchange. To further understand the pathological mechanisms underlying progressive emphysema, we used MS-based approaches to quantify the lung, bronchoalveolar lavage fluid (BALF) and serum metabolome during emphysema progression in the established murine porcine pancreatic elastase (PPE) model on days 28, 56 and 161, compared with PBS controls. Partial least squares (PLS) analysis revealed greater changes in the metabolome of lung followed by BALF rather than serum during emphysema progression. Furthermore, we demonstrate for the first time that emphysema progression is associated with a reduction in lung-specific L-carnitine, a metabolite critical for transporting long-chain fatty acids into the mitochondria for their subsequent  $\beta$ -oxidation. In vitro, stimulation of the alveolar epithelial type II (ATII)-like LA4 cell line with L-carnitine diminished apoptosis induced by both PPE and  $H_2O_2$ . Moreover, PPE-treated mice demonstrated impaired lung function compared with PBS-treated controls (lung compliance;  $0.067 \pm 0.008$  ml/cm $H_2O$  compared with  $0.035 \pm 0.005$  ml/cm $H_2O$ , P < 0.0001), which improved following supplementation with L-carnitine ( $0.051 \pm 0.006$ , P < 0.01) and was associated with a reduction in apoptosis. In summary, our results provide a new insight into the role of L-carnitine and, importantly, suggest therapeutic avenues for COPD.

Key words: apoptosis, biomarkers, chronic obstructive pulmonary disease (COPD), metabolome.

# INTRODUCTION

Chronic obstructive pulmonary disease (COPD), a leading cause of chronic morbidity and mortality worldwide, is the result of long-term exposure to toxic gases and particles, in particular cigarette smoke, which drives excess mucus production, small airway remodelling, chronic bronchitis and emphysema [1]. Emphysema is the destruction of septal tissue, leading to enlarged airspaces and reduced surface area [2]. Historically, the underlying mechanism of emphysema has been viewed as

a protease/anti-protease imbalance resulting in loss of the alveolar wall matrix [3], indeed patients with  $\alpha_1$ -antitrypsin deficiency have an increased risk of emphysema development [4]. More recently, oxidative stress [5], accelerated senescence [6] and an apoptosis/proliferation imbalance of both alveolar epithelial and endothelial cells [7,8] have been described as being responsible for the development of emphysema. These pathological changes result in a progressive airflow limitation that is not fully reversible. Indeed, there is no curative therapy for COPD, with currently available treatment only able to alleviate

Abbreviations: ATII, alveolar epithelial type II; AUC, area under the curve; BALF, bronchoalveolar lavage fluid; COPD, chronic obstructive pulmonary disease; H&E, haematoxylin and eosin; HRP, horseradish peroxidase; MAPK, mitogen-activated protein kinase; MLI, mean linear intercept; PC, phosphatidylcholine; PI, propidium iodide; PLS, partial least squares; PPE, porcine pancreatic elastase; ROC, receiver operating characteristic; SM, sphingomyelin; TLC, total lung capacity.

Correspondence: Dr Ali Önder Yildirim (email oender.yildirim@helmholtz-muenchen.de).

symptoms. Furthermore, little is known about the factors actually driving COPD disease progression towards a particular phenotype with progression among individual patients being highly variable.

Metabolomics, a rapidly expanding field which can be described as profiling the metabolic pathways of cells, offers a powerful tool for assessing the physiological state of an individual yielding a snapshot of cellular activities closer to the phenotype than simply gene expression [9], thus providing an invaluable resource for identifying new biomarkers of disease progression and further elucidating the underlying pathophysiological mechanisms of disease development, most importantly, to potentially reveal new therapeutic targets. To this end, there have been a number of studies published over the last few years assessing the COPD metabolome. This has included both untargeted [10-13] and targeted [14] metabolomics, as well as a combination of both [15] measured in either plasma or serum from COPD patients. In their combined approach, Bowler et al. [15] reported a strong inverse association between the level of some plasma sphingomyelins (SMs) and emphysema in COPD patients. In addition to these clinical studies, one animal study used an untargeted approach to examine metabolomic changes in plasma following chronic exposure to cigarette smoke in a mouse model that resulted in emphysema [16] and a very recent study examining the effect of traditional Chinese medicine on a cigarette-smoke-induced rat model of COPD examined metabolite levels in lung tissue [17]. However, to the best of our knowledge, no study has yet assessed the metabolomic changes occurring in the emphysematous lung during disease progression.

In the present study, for the first time, we use targeted metabolomics to assess changes in the metabolome locally to the lung and systemically in serum during disease progression, using the well-established porcine pancreatic elastase (PPE)-induced model of murine emphysema [18,19]. We demonstrated that the progression of emphysema is associated with reduced levels of Lcarnitine in the lung. L-Carnitine's primary function is to transport long-chain fatty acids into the mitochondria for their subsequent  $\beta$ -oxidation and energy production [20], but it is also a widely known antioxidant and protector against apoptosis [21-26]. Interestingly, it has also been suggested following a randomized double-blind trial that L-carnitine supplementation improved the control of asthma in children suffering from moderate persistent disease [27], which has been supported by an in vivo study in mice using the ovalbumin model of asthma tentatively reporting that L-carnitine treatment improved oxygen saturation and improved bronchus-associated inflammation [28]. Furthermore, L-carnitine supplementation as an ergogenic aid for COPD patients undergoing whole-body and respiratory muscle training programmes demonstrated improved exercise tolerance and inspiratory muscle strength [29]. However, a mechanism of action for the potential benefits of L-carnitine on lung pathology is also yet to be elucidated. To overcome these limitations and further investigate the interaction of metabolomics with the progression of emphysema development, we used MS-based approaches to quantify the lung, bronchoalveolar lavage fluid (BALF) and serum metabolome at three different time points during emphysema progression. Furthermore, we integrate systems biological approaches with well-known metabolomics profiling to discover relationships that might elucidate mechanisms of progression in emphysema development. Therefore we hypothesized that supplementing mice with L-carnitine may protect against the development of PPE-induced emphysema. L-Carnitine protected alveolar cells *in vitro* from PPE-induced apoptosis. Furthermore, supplementation of mice *in vivo* with L-carnitine prevented the development of alveolar apoptosis that is associated with emphysema and significantly improved the lung function of mice exposed to PPE. These findings suggest that L-carnitine supplementation, which is used clinically for the treatment of newborns with congenital metabolic diseases [30], may be beneficial to COPD patients.

# **MATERIALS AND METHODS**

#### **Animals**

Female C57BL/6N mice (Charles River Laboratories) aged 8-10 weeks were exposed oropharyngeally to a single application of 80 units of PPE/kg of body weight (Sigma–Aldrich) in an 80  $\mu$ l volume. Control mice were treated with 80 µ1 of PBS (Gibco Life Technologies). Mice were analysed on days 28, 56 and 161 for lung function, lung morphology and metabolomics profiling (n = 6-11 per group). In further experiments, mice were additionally treated every second day i.p. with 500 mg of L-carnitine/kg of body weight (Sigma-Aldrich) and analysed on day 28 (n = 46, experiment repeated twice). Mice were housed under specific pathogen-free conditions, exposed to a 12-h light/12-h dark cycle with access to food and water ad libitum, in rooms maintained at a constant temperature and humidity. All animal experiments were performed according to strict governmental and international guidelines and were approved by the local government for the administrative region of Upper Bavaria.

#### **Lung function measurement**

Mice were anaesthetized with ketamine/xylazine and tracheostomized, and their pulmonary function was analysed using the flexiVent system (Scireq). To obtain a mean lung volume similar to that of spontaneous breathing, mice were ventilated with a tidal volume of 10 ml/kg at a frequency of 150 breaths/min. Lung mechanical properties were tested using the SnapShot and Primewave perturbations. Four readings per animal were taken.

### Bronchoalveolar lavage fluid and serum

BALF was obtained for metabolomics analysis and to undertake total and differential cell counts for inflammatory cell recruitment of macrophages, neutrophils and lymphocytes. The lungs were lavaged three times with 500  $\mu l$  of PBS. Cells were pelleted at 400 g, supernatant was stored at  $-80\,^{\circ}\mathrm{C}$  for further analysis and the cells were resuspended in RPMI 1640 medium (Gibco Life Technologies) for the total cell count using a haemocytometer. Cytospins of the cell suspension were then prepared and stained using May–Grünwald–Giemsa for differential cell counting (200 cells/sample) using morphological criteria [31].

Serum was collected for metabolomics analysis. Mice were bled from the femoral artery, blood was left to clot for several hours and was then centrifuged at 1300 g for 15 min, serum was divided into aliquots and stored at -80 °C for further analysis.

#### Lung processing

The right lung was snap-frozen in liquid nitrogen for further analysis. The left lung was fixed under a constant pressure of 20 cm H<sub>2</sub>O by intra-tracheal instillation of 6% paraformaldehyde and using systematic uniform random sampling embedded into paraffin for haematoxylin and eosin (H&E)-stained histological analysis and immunohistochemistry. Images of stained sections were obtained using a Mirax Desk (Carl Zeiss MicroImaging) slide scanner and analysed using Pannoramic Viewer version 1.15.2 (3DHistech Kft).

# **Quantitative morphometry**

H&E-stained lung tissue sections were analysed by design-based stereology using an Olympus BX51 light microscope equipped with the new Computer Assisted Stereological Toolbox (new-CAST, Visiopharm) as described previously [32]. Air space enlargement was assessed by calculating the mean linear intercept (MLI) across 30 random fields of view per lung. Lung section images were superimposed with a line grid, the intercepts of lines with alveolar septa and points hitting airspace were counted to calculate the MLI, using  $\text{MLI} = \sum P_{\text{air}} \times L(\text{p})/\sum I_{\text{septa}} \times 0.5$ , where  $P_{\text{air}}$  are the points of the grid hitting airspaces, L(p) is the line length per point, and  $I_{\text{septa}}$  is the sum of intercepts of alveolar septa with grid lines.

To quantify the percentage of caspase 3-positive alveolar epithelial cells the immunohistochemically stained lung tissue sections were also analysed using the newCAST system. Thirty random fields of view per lung were taken and a frame grid was superimposed on lung section images taken with the  $\times$  40 objective. Within the frame, alveolar epithelial cells positive or negative for caspase 3 staining were counted and the percentage of positive alveolar epithelial cells was calculated.

## **Targeted metabolomics**

Targeted metabolomics screening using the Absolute IDQ<sup>TM</sup> p180 Kit (BIOCRATES Life Sciences) followed by mass spectrometric analysis of serum, BALF and lung homogenate was undertaken by the Metabolomics Platform of the Genome Analysis Centre of the Helmholtz Zentrum München. For serum and BALF,  $10~\mu l$ of sample, and for lung tissue, 10  $\mu$ l of homogenate supernatant, was applied to the kit plate. The tissue homogenate was prepared using a Precellys 24 homogenizer with an integrated cooling unit and homogenization tubes with ceramic beads (1.4 mm). To each milligram of frozen lung tissue, 3  $\mu$ l of a dry ice-cooled mixture of ethanol/phosphate buffer [85:15 (v/v)] was added. The measurements with the AbsoluteIDQTM kit p180 and the preparation of tissue samples have been previously described in detail [33,34]. Sample handling was performed with a Hamilton Microlab STAR<sup>TM</sup> robotics system (Hamilton Bonaduz). Samples were analysed on an API4000<sup>TM</sup> LC/MS/MS system (AB Sciex Deutschland). Data evaluation to quantify the metabolite concentrations was performed with the MetIQ<sup>TM</sup> software package, which is an integral component of the AbsoluteIDQ<sup>TM</sup> kit. Concentrations of all metabolites were calculated using internal

standards and reported in  $\mu$ mol. Further analyses on the data set were performed with MATLAB version 8.1.0.604 (R2013a; MathWorks) using the Statistics Toolbox version 8.2 and libPLS version 1.95 [35].

In total, 186 metabolites are quantified by the kit: 40 acylcarnitines ( $C_{x:y}$ ) including free carnitine ( $C_0$ ), 21 amino acids, 19 biogenic amines, 90 glycerophospholipids including lysophosphatidylcholines (lysoPC a  $C_{x:y}$ ), diacylphosphatidylcholines (PC aa  $C_{x:y}$ ) and acyl-alkyl phosphatidylcholines (PCs ae  $C_{x:y}$ ), 15 sphingolipids including SM ( $C_{x:y}$ ) and hydroxysphingomyelins [SM (OH)  $C_{x:y}$ ] and hexose (sugars with six carbons). The abbreviation  $C_{x:y}$  is used to denote the lipid side chain composition, x and y refer to the total number of carbons and double bonds respectively, as the MS technology used cannot distinguish between the side chains of diacylphospholipids. Acyl side chains are abbreviated with an 'a', alkyl and alkenyl residues with an 'e'. Side chain substitutions are indicated as follows: hydroxy- (OH), methyl- (M) and dicarboxy- (DC).

### L-Carnitine quantification of lung tissue

Free L-carnitine levels were quantified in lung tissue using the L-Carnitine Assay Kit (Sigma—Aldrich) as per the manufacturer's instructions. In brief, lung tissue was homogenized under liquid nitrogen using the Mikro-Dismembrator S (Sartorius) and extracted into Carnitine Assay Buffer. Reactions were prepared as described in the kit with each sample being analysed in triplicate. To control for background readings from CoA, a blank sample omitting the Carnitine Converting Enzyme Mix was prepared. After incubation, absorbance was measured at 570 nm on a Microplate reader (Infinite M200 PRO NanoQuant; Tecan Deutschland). L-Carnitine concentration was calculated from kit standards and normalized to the protein concentration as determined by the Pierce BCA protein Assay Kit (Thermo Fisher Scientific).

#### **Immunohistochemistry**

Paraffin-embedded lung sections were first deparaffinized in xylene and rehydrated in alcohol before being treated with 1.8% (v/v) H<sub>2</sub>O<sub>2</sub> solution (Sigma-Aldrich) to block endogenous peroxidase activity. Heat-induced epitope retrieval was undertaken using HIER citrate buffer (pH 6.0, ZYTOMED Systems) in a decloaking chamber (Biocare Medical). Sections were then blocked using Rodent Blocking Buffer (Biocare Medical), before being incubated overnight at 4°C with a primary antibody against cleaved caspase 3 (1:500 dilution, AP21655SU-S, Acris Antibodies). These were then incubated with an alkaline phosphataselabelled secondary antibody (Biocare Medical) for 1 h at room temperature and then the signal was amplified with the chromogen substrate Vulcan Fast Red (Biocare Medical). Sections were counterstained with haematoxylin (Sigma-Aldrich), dehydrated in xylene and coverslips were mounted with Entellan (Merck Millipore).

#### Western blot analysis

Samples of 20  $\mu$ g of protein were resolved by SDS/PAGE and transferred on to a PVDF membrane (Bio-Rad Laboratories). The membrane was blocked with 5% non-fat dried skimmed milk powder and immunoblotted overnight at 4°C with anti cleaved

caspase 3 (AP21655SU-S, Acris Antibodies). Antibody binding was detected with a horseradish peroxidase (HRP)-conjugated goat anti-rabbit IgG (ab6721, Abcam) followed by developing with ECL Prime Reagent (GE Healthcare). Bands were detected and quantified using the Chemidoc XRS system (Bio-Rad Laboratories) and normalized to  $\beta$ -actin levels (HRP-conjugated anti- $\beta$ -actin mouse monoclonal antibody, A3854, Sigma–Aldrich).

# LA4 cell apoptosis assay

The murine alveolar epithelial type II (ATII)-like cell line LA4 (A.T.C.C.) was maintained in Ham's F12 medium containing NaHCO3 and stable glutamine (Biochrom), supplemented with 15% FBS (Gibco Life Technologies), 100 units/ml penicillin/streptomycin (Sigma-Aldrich) and 1% non-essential amino acids (Biochrom) at 37 °C in a 5 % CO<sub>2</sub> atmosphere. Cells were trypsinized (trypsin/EDTA solution, Sigma-Aldrich) and seeded at  $6 \times 10^4$  cells per well in 24-well plates. After 24 h, cells were cultured in serum-free maintenance medium containing increasing concentrations (0–1 mM) of L-carnitine (Sigma–Aldrich) for a further 24 h. Apoptosis was induced by treating with either 0.5 units/ml PPE for 6 h in serum-free maintenance medium or pulsed with 500  $\mu$ M H<sub>2</sub>O<sub>2</sub> (Sigma–Aldrich) for 1 h followed by 48 h of incubation in full maintenance medium supplemented with increasing concentrations (0–1 mM) of L-carnitine (Sigma– Aldrich). Apoptosis levels were analysed using the Annexin V Apoptosis Detection Kit APC (eBioscience) as per the manufacturer's instructions and the stained cells quantified with a BD FACSCanto II flow cytometer (BD Biosciences) and BD FAC-SDiva software.

## Analysing superoxide production

MitoSOX Red (Life Technologies) was used to analyse the level of mitochondrial superoxide production in LA4 cells. Briefly, LA4 cells seeded at  $2\times10^5$  cells per well in 12-well plates were cultured for 24 h in full maintenance medium. Cells were then cultured for a further 24 h in serum-free maintenance medium containing increasing concentrations (0–1 mM) of L-carnitine (Sigma–Aldrich). Cells were pulsed with  $\rm H_2O_2$  for 1 h and then incubated for a further 6 h in serum-free maintenance medium. After which they were stained on the plate with medium containing 5  $\mu$ M MitoSOX Red. Cells were washed with PBS, trypsinized and resuspended in PBS + 0.5 % BSA for analysis on a BD FACSCanto II flow cytometer (BD Biosciences). Superoxide production was measured as mean MitoSOX fluorescence intensity in the PE channel.

#### Statistical analysis

All data analysis, unless indicated otherwise, was undertaken using GraphPad Prism version 6 (GraphPad Software). Results are presented as mean values  $\pm$  S.D. All experiments that contained more than two groups were analysed using one-way ANOVA followed by Bonferroni's post-hoc testing.

#### **RESULTS**

# Targeted metabolite screening of serum, BALF and lung from emphysematous mice

Intra-tracheal instillation of PPE in mice is known to cause airspace enlargement with breaks in the alveolar wall compatible with destruction [36]; which is comparable to emphysema in COPD patients. Despite PPE being shown to be cleared from the lungs of rodents within 24 h [37], airspace enlargement continues long after this time [18,36]; indeed we have recently shown emphysema following a single oropharangeal application of PPE to continue progressing to day 161 [19]. Figure 1(A) clearly demonstrates a time-dependent enlargement of the airspaces in H&Estained lung sections from PPE-treated mice compared with control animals. Lung function analysis of the same mice revealed a time-dependent progression in both increasing lung compliance and total lung capacity (TLC; 0.072 ± 0.0096 ml/cmH<sub>2</sub>O compared with  $0.110 \pm 0.0092 \text{ ml/cmH}_2\text{O}$ , P < 0.0001 for compliance and  $1.01 \pm 0.08$  ml compared with  $1.30 \pm 0.09$  ml, P < 0.0001 for TLC, of PPE-treated mice at days 28 and 161 post-exposure respectively) and a reduction in tissue elastance  $(10.08 \pm 1.75 \text{ cmH}_2\text{O/ml} \text{ compared with}$  $6.86 \pm 0.63$  cmH<sub>2</sub>O/ml, P < 0.01, for PPE-treated mice at days 28 and 161 post-exposure respectively) following a single application of PPE (Figure 1B), thus further confirming the development of progressive emphysema in mice treated with a single dose of PPE. Differential cell counts of cytospins obtained from the BALF confirmed that, at later time points, emphysema was progressing independently of inflammation in the PPE-treated mice (Figure 1C). Indeed, only at day 28 was there a slight increase in the BALF macrophage number of PPE-treated mice that had returned to baseline by day 56. This model therefore provides a great platform to assess potential changes in the mouse metabolome that are occurring during disease progression.

To assess changes in the mouse metabolome during emphysema development, serum, BALF and homogenized lung tissue taken at days 28, 56 and 161 from mice exposed to a single application of PPE and their respective PBS controls were analysed using the AbsoluteIDQTM p180 Kit (Biocrates Life Sciences) that targets acylcarnitines, amino acids, biogenic amines, glycerophospholipids, sphingolipids and hexose. A heat map representation of the significantly changed metabolites across the different tissue types following the application of PPE, at the three time points examined, is shown in Figure 2(A). Immediately apparent, perhaps not unsurprisingly, is the increase in the number of metabolites that change as the disease progresses, especially from day 28 to day 56, with most metabolites being down-regulated. Interestingly, a significantly reduced level in a large number of the PC family members is observed in both the BALF and the lung tissue, particularly in BALF during the progression of emphysema (Figure 2A). As proof of principle, a reduction in PC has previously been reported in the BALF of emphysema patients and from airway epithelial cells isolated from mice exposed to cigarette smoke for 8 weeks

In a recent study, an inverse association between the level of certain plasma SM and emphysema in COPD patients was de-

L-Carnitine attenuates emphysema Original Paper

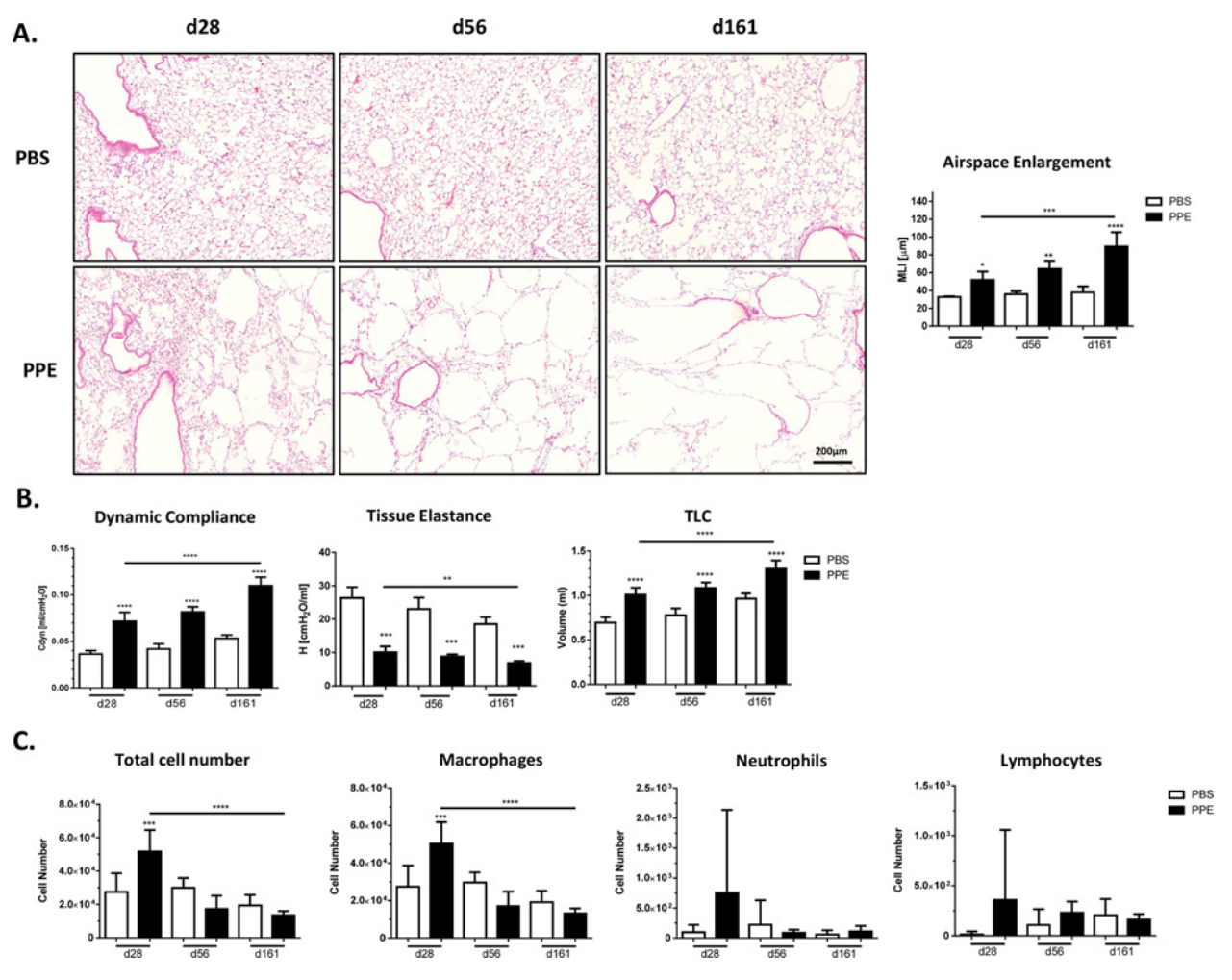


Figure 1 A single oropharyngeal application of PPE leads to the development of progressive emphysema in the lungs of mice

(A) Representative photomicrographs of H&E-stained lung sections from PBS- and PPE-treated mice at the time points indicated. Scale bar =  $200~\mu m$ . Airspace enlargement was quantified as the MLI by design-based stereology using the newCAST system. (B) Lung function measurements to obtain TLC, tissue elastance and dynamic compliance in PBS- and PPE-treated mice at the time points indicated. (C) Total and differential cell counts in the BALF. Data shown are from one experiment with six to 11 mice per group at each time point, with mean values  $\pm$  S.D. given. One-way ANOVA followed by Bonferroni's post-hoc test with \*P < 0.05, \*\*P < 0.01, \*\*\*P < 0.001, \*\*\*\*P < 0.0001.

scribed [15]. Although we saw no significant change in serum SM levels in our mouse model of emphysema, a number of SMs were significantly reduced during the progression of emphysema more local to the lung (Figure 2A). In the BALF, palmitoylsphingomyelin (SM  $C_{16:0}$ ), palmitoleic sphingomyelin (SM  $C_{16:1}$ ), lignoceroylsphingomyelin (SM  $C_{24:0}$ ) and nervonicsphingomyelin (SM  $C_{24:1}$ ) were reduced at all three time points examined as well as stearoylsphingomyelin (SM  $C_{18:0}$ ) and lignoceroylsphingomyelin (SM  $C_{24:0}$ ) in lung tissue from day 56 onwards (Figure 2A). These results provide lung-specific information on SM levels and emphysema progression that was lacking from the patient study.

Furthermore, Figure 2(A) also indicates that the pattern of altered metabolites is very compartment specific, with greater changes detectable locally to the lung in both the homogenized tissue and the BALF. This was confirmed in a 2D partial least

squares (PLS) analysis [40] of all metabolites using samples from all mice adjusted for time effect. The PLS revealed that there were major differences in mean metabolite concentrations between PBS- and PPE-treated mice mainly in the lung tissue and BALF, as can be seen from the first two PLS components separating the two groups almost perfectly in those two tissues and not to the same extent in serum (Figure 2B). To validate the performance of this classification receiver operating characteristic (ROC) curves were generated from 5-fold cross-validation and the area under the curve (AUC) was calculated. Figure 2(C) depicts the mean ROC curves from 5-fold cross-validation for all three tissue types plus a reference curve, with an AUC of 0.5, highlighting how a random assignment to treatment groups would appear. With an AUC of 1.0, lung tissue perfectly separates PPE from PBS-treated mice, BALF (AUC of 0.96) also shows a high level of separation between the two treatment groups, whereas

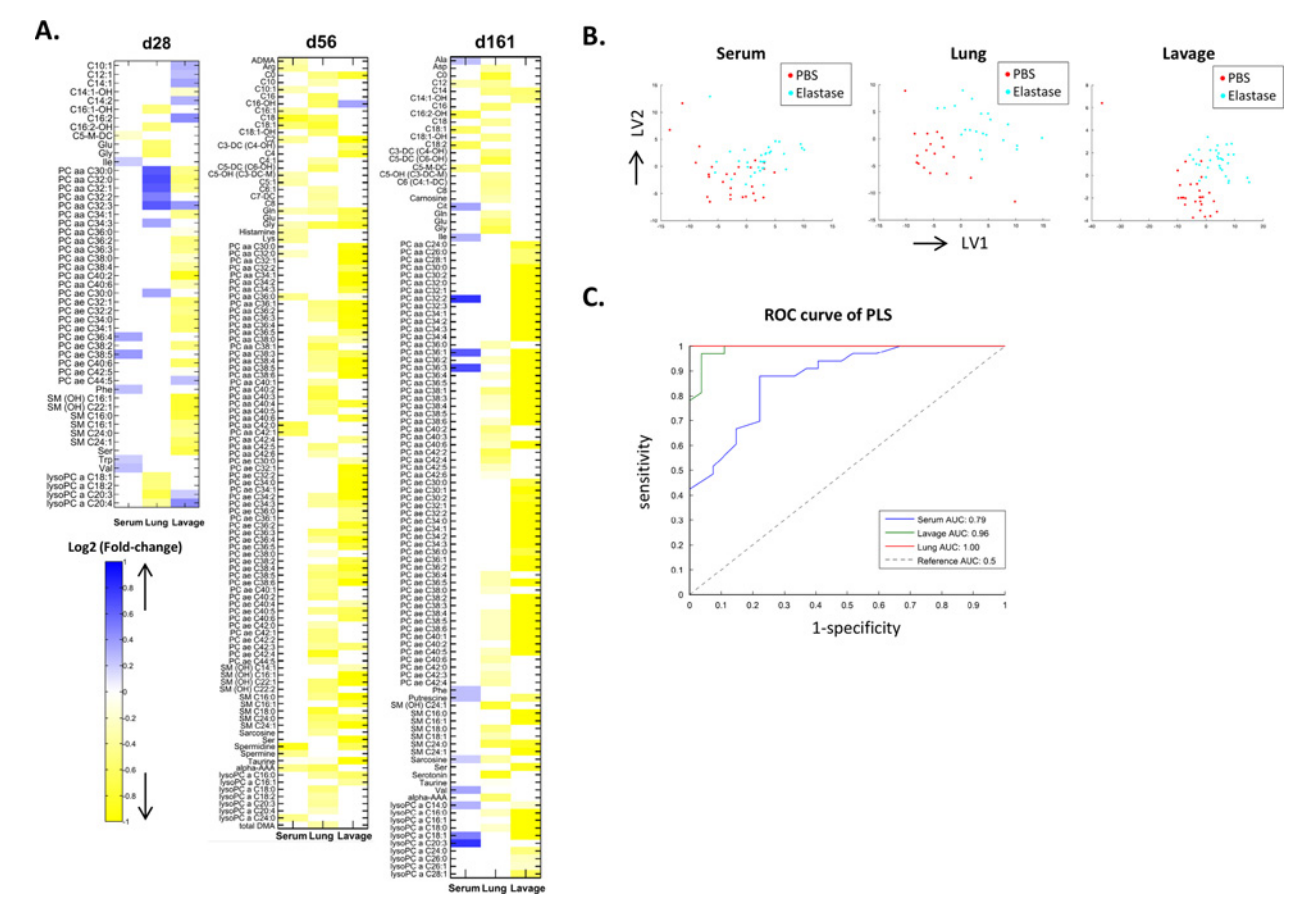


Figure 2 Targeted metabolomics reveals that there are greater changes in the metabolome local to the lung than in the serum during the progression of PPE-induced emphysema

Metabolomics screening using the Absolute/ $DQ^{TM}$  p180 Kit followed by mass spectrometric analysis of serum, BALF and lung homogenate was undertaken on the mice described in Figure 1. (**A**) Heat maps demonstrating the mean relative fold change in individual metabolite concentrations in mice exposed to PPE compared with PBS controls at the time points indicated. A white box means the metabolite was not significantly altered in that tissue at that time point (P > 0.05, Student's t test) following univariate analysis. A blue box represents an increase in the metabolite and yellow a decrease. (**B**) 2D PLS analyses of all metabolites in all mice at every time point. Each dot represents an individual mouse. LV, latent variable. (**C**) ROC curve generated from 5-fold cross-validation of the PLS analysis. A representative model for each tissue type is shown plus a reference curve, along with the AUC.

serum shows the least level of separation with an AUC of 0.79 (Figure 2C). Taken together, these data suggest that emphysema progression is associated with a reduction in the global metabolomic profile and that this is compartment-specific, with most changes being detectable locally to the lung. Furthermore, we confirm previous findings that PC is reduced in the BALF and extend the previously published observation that demonstrated an inverse association between the level of certain plasma SM and emphysema, by extending this finding to the lung tissue and BALF, thus suggesting the PPE-induced murine model of emphysema to be a good model of disease progression for further elucidating the underlying molecular mechanisms.

# Lung L-carnitine levels are significantly reduced during emphysema

The PLS analysis revealed the greatest level of separation in the metabolomics profile between the PBS- and PPE-treated groups to be in the lung tissue. Based on this finding, we decided to focus in the present study only on changes in the emphysematous metabolome that were local to the lung. In Figure 3(A), we depict the total concentration of lung metabolites stratified by their family class. There was a significant reduction in the concentration of acylcarnitines and amino acids especially at days 56 and 161 post-PPE treatment, with biogenic amines and lysophosphatidylcholines also showing a reduction to a lower extent (Figure 3A). In order to examine these changes more closely, we analysed the lung data as volcano plots of mean fold change compared with  $-\log_{10}(P\text{-value})$  of individual metabolites (Figure 3B). This revealed an intriguing target, i.e. L-carnitine, highlighted with a red circle on the volcano plots. In the lung tissue at day 56 post-PPE treatment L-carnitine was one of the more significantly regulated metabolites, but by day 161 it had become the most significantly regulated metabolite in the lung (Figure 3B). Specifically, the concentration of L-carnitine in the lung tissue at all time points examined shows that the reduction in the concentration of total acylcarnitines, was predominantly due to a

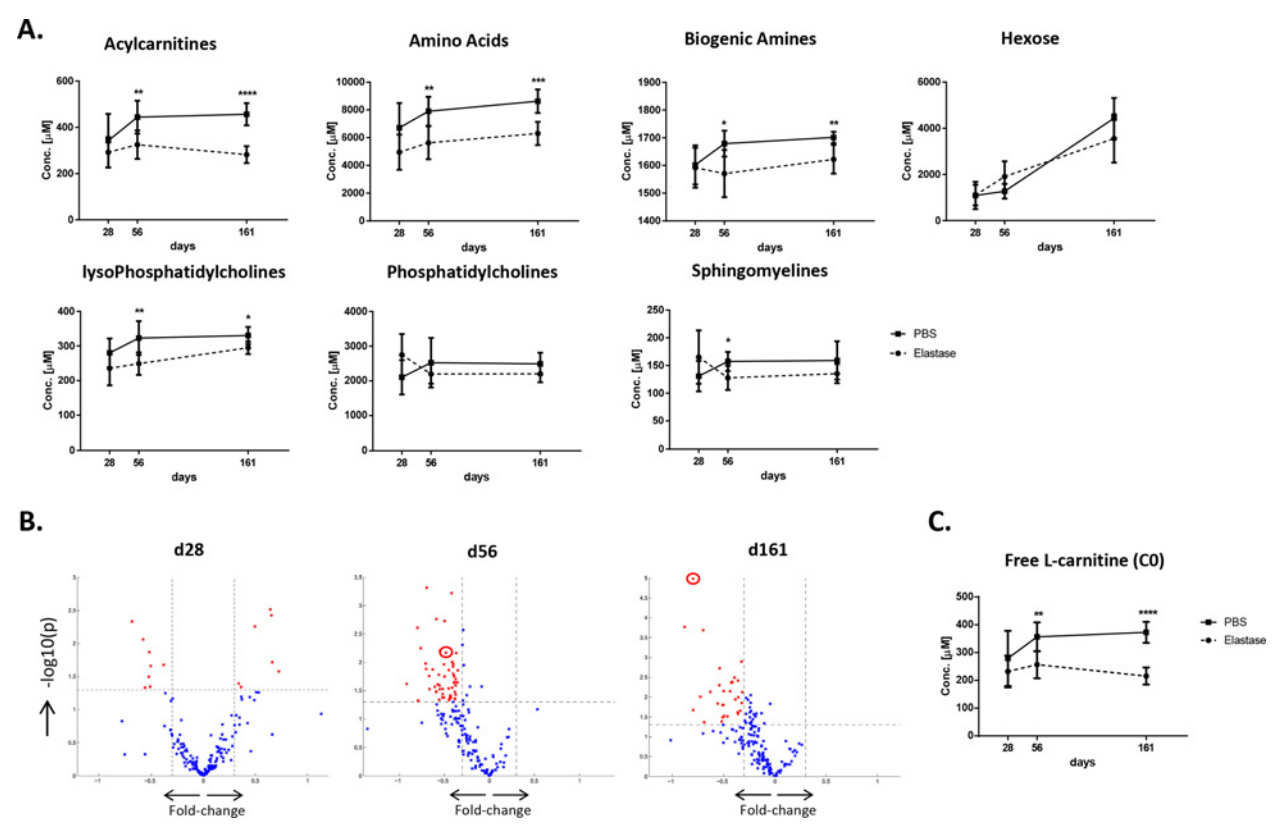


Figure 3

L-Carnitine is the most significantly altered lung metabolite during emphysema progression

(A) The totals of the concentration of lung tissue metabolites detected within the class indicated, at the time points shown.

(B). A plot of the mean log₂(relative fold change) compared with −log₁₀(P) for each individual metabolite at the time point indicated in lung tissue, from PPE-treated mice compared with PBS controls. Significance was taken as P < 0.05 (Student's t test) and a fold change > 0.3 in either direction, as indicated by the red data points and hatched lines. Free L-carnitine (CO) is highlighted by a red circle. (C) The concentration of free L-carnitine (CO) in lung tissue. Data shown are the mean values ± S.D. from six to 11 mice per group at each time point taken from the Absolute/DQ™ p180 metabolomics screen, with \*P < 0.05, \*\*P < 0.01, \*\*\*P < 0.001, \*\*\*\*P < 0.0001 following Student's t test.

reduction in the level of free L-carnitine (372.71  $\pm$  38.11  $\mu$ M compared with 215.50  $\pm$  30.46  $\mu$ M, P < 0.001, PBS- compared with PPE-treated mice at day 161; Figure 3C). Our findings show for the first time that L-carnitine reduction predisposed to the progression of elastase-induced emphysema development.

# L-Carnitine protects alveolar epithelial type II cells from apoptosis

The enlarged airspaces and reduced surface area characteristic of emphysema is caused by the destruction and loss of alveolar structures, accompanied by increased levels of apoptosis in alveolar epithelial cells [7,8]. Previous studies in a variety of cell types have reported that L-carnitine protected against oxidative stress, improved mitochondrial function and inhibited apoptosis development [21–26], and, interestingly, treatment of the human lung epithelial cell line A549 with L-carnitine reversed amiodarone-induced loss of cellular ATP and mitochondrial membrane depolarization [41]. We therefore investigated the protective effects of L-carnitine *in vitro* on PPE-induced apoptosis of the murine alveolar epithelial type II-like cell line LA4. We first determined whether PPE could induce apoptosis of LA4

cells. Figure 4(A) highlights a dose-dependent increase in the level of apoptosis following 6 h incubation with increasing concentrations of PPE as determined by flow cytometry of annexin V and propidium iodide (PI)-stained LA4 cells (14.17  $\pm$  2.14% compared with 46.80 + 13.10% annexin V<sup>+</sup> PI<sup>+</sup> cells, P < 0.001, 0 unit/ml compared with 1 unit/ml PPE). Further analysis defined that culturing LA4 cells in the presence of L-carnitine up to concentrations of 1 mM for up to 72 h had no detrimental impact on cell viability as determined by flow cytometry of annexin V<sup>-</sup> and PI<sup>-</sup> cells (Figure 4B). Pre-culturing the LA4 cells with increasing concentrations of L-carnitine for 24 h subsequently reduced the level of apoptosis detected following 6 h incubation with 0.5 unit/ml PPE (Figure 4C). Examining the data closely, we observed an overall increase in live cells (29.78  $\pm$  10.05 % compared with  $56.30 \pm 3.00 \%$  annexin V<sup>-</sup> PI<sup>-</sup> cells, P < 0.01, 0 mMcompared with 1 mM L-carnitine) and a reduction in total apoptotic cells (47.13  $\pm$  12.35% compared with 28.83  $\pm$  2.29% annexin  $V^+$  cells, P < 0.05), but there was a slight increase in early apoptotic cells following pre-treatment with 1 mM L-carnitine  $(6.50 \pm 2.90\,\%$  compared with  $13.28 \pm 2.67\,\%$  annexin  $V^+$   $PI^$ cells, P < 0.01). This is, however, offset by a reduction in the

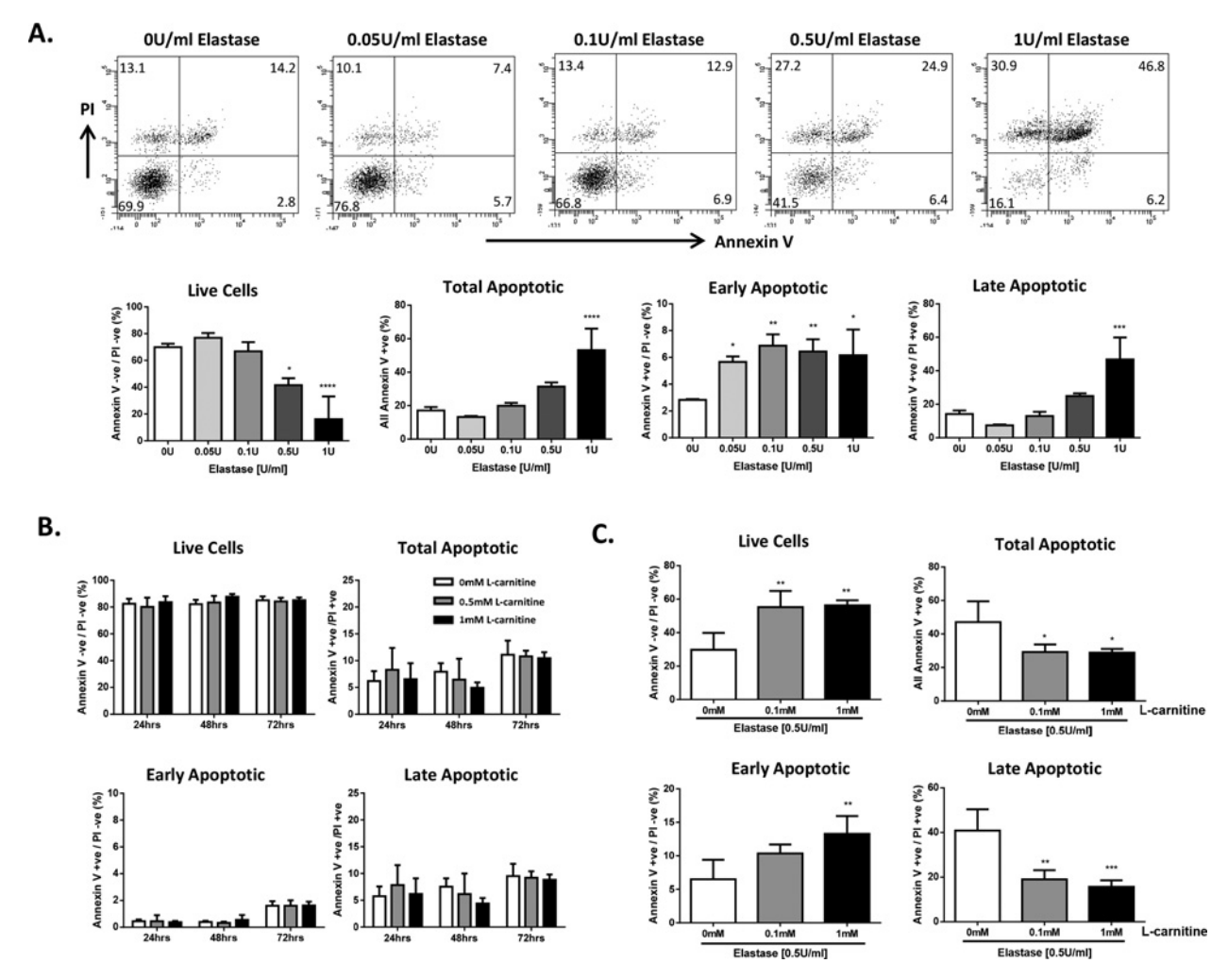


Figure 4 Pre-treatment with L-carnitine protects LA4 cells from PPE-induced apoptosis (A) The ATII-like cell line LA4 was cultured with increasing concentrations of PPE for 6 h and then the level of apoptosis was determined by staining with annexin V and PI, followed by flow cytometric analysis. Representative FACS plots are demonstrated, with mean quadrant values indicated. Data shown are the percentages of cells (means  $\pm$  S.D.) from the following quadrants: live cells, annexin V $^-$  PI $^-$ ; total apoptotic, all annexin V $^+$  cells; early apoptotic, annexin V $^+$  PI $^-$ ; late apoptotic, annexin V $^+$  PI $^+$ . (B) LA4 cells were cultured with increasing concentrations of L-carnitine for the time points shown and viability determined as in (A). (C) LA4 cells were cultured for 24 h in the presence of L-carnitine at the concentrations shown followed by 6 h of incubation with PPE at a concentration of 0.5 unit/ml. The level of apoptosis was determined as in (A). For all charts, mean values  $\pm$  S.D. from one representative experiment (n = 3-4) repeated two to three times are shown. One-way ANOVA followed by Bonferroni's post-hoc test was undertaken with \* $^+$ P < 0.005, \* $^+$ P < 0.001, \* $^+$ \*\* $^+$ P < 0.0001, \* $^+$ \*\* $^+$ P < 0.0001 compared with the control group.

number of late apoptotic cells ( $40.88 \pm 9.50\%$  compared with  $15.70 \pm 2.89\%$ , annexin V<sup>+</sup> PI<sup>+</sup> cells, P < 0.001, 0 mM compared with 1 mM L-carnitine).

It has previously been shown that  $H_2O_2$ -induced apoptosis of alveolar epithelial type II cells proceeds through a mechanism of increased intracellular oxidants, mitochondrial membrane depolarization, cytochrome c release and caspase activation [42]. Interestingly, ceramide signalling has also been reported to act as the second messenger in  $H_2O_2$ -induced apoptosis of human airway epithelial cells [43], and up-regulation of ceramide has been associated with pulmonary cell apoptosis in emphysema [44]. We therefore examined the ability of L-carnitine to inhibit  $H_2O_2$ -induced apoptosis of LA4 cells. LA4 cells were cultured in

the presence of increasing concentrations of L-carnitine for 24 h, pulsed for 1 h with 500  $\mu$ M  $\rm H_2O_2$  and then cultured for a further 48 h with L-carnitine. Figure 5(A) clearly shows a dose-dependent reduction in the number of both early (25.55  $\pm$  3.41% compared with  $8.48\pm3.60$ % annexin  $\rm V^+$   $\rm PI^-$  cells, P<0.0001,~0 mM compared with 1 mM L-carnitine) and late (54.10  $\pm$  3.27 compared with 23.58  $\pm$  11.04 annexin  $\rm V^+$   $\rm PI^+$  cells, P<0.001,~0 mM compared with 1 mM L-carnitine) apoptotic LA4 cells, with a concomitant increase in live cells, when cultured in the presence of elevated concentrations of L-carnitine. To assess levels of mitochondrial superoxide, as a marker of reactive oxygen species production, we stained LA4 cells with the mitochondria-specific probe MitoSOX Red. Staining with MitoSOX Red revealed that

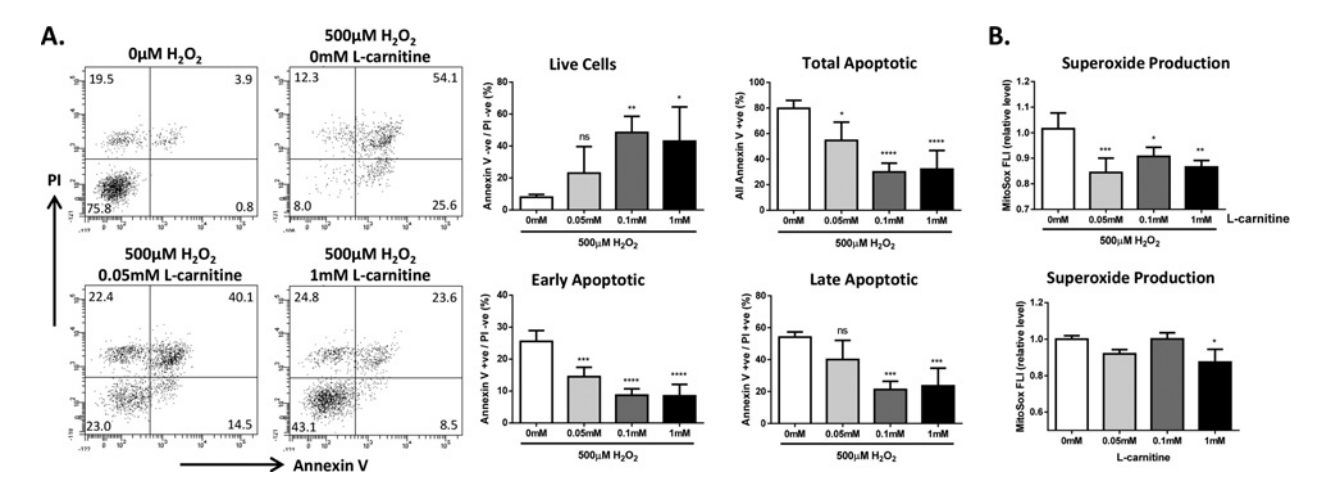


Figure 5  $H_2O_2$ -induced apoptosis of LA4 cells is prevented by pre-treatment with L-carnitine (A) LA4 cells were cultured for 24 h in the presence of L-carnitine at the concentrations shown, followed by a 1-h pulse with 500  $\mu$ M  $H_2O_2$ ; cells were then cultured for a further 48 h before analysis. The level of apoptosis was determined as described in Figure 4(A). Data shown are means  $\pm$  S.D. from one representative experiment (n = 4) repeated three times. (B) LA4 cells were cultured for 24 h in the presence of L-carnitine at the concentrations shown; some cells were also pulsed with 500  $\mu$ M  $H_2O_2$  for 1 h, as indicated; all cells were then cultured for further 6 h before analysis. Data shown are the relative MitoSOX fluorescence intensities of treated groups compared with control, means  $\pm$  S.D., from one representative experiment, n = 3-4, repeated twice. For all charts, one-way ANOVA followed by Bonferroni's post-hoc test was undertaken with \*P < 0.05, \*P < 0.01, \*P < 0.001, \*P < 0.001 compared with the control group.

L-carnitine protection against  $H_2O_2$ -induced apoptosis was accompanied by reduced generation of mitochondrial superoxide (Figure 5B), in keeping with the proposed antioxidant function of L-carnitine. Interestingly, culturing LA4 cells in the presence of L-carnitine without  $H_2O_2$  treatment also significantly reduced the level of mitochondrial superoxide, but only at the highest dose examined.

Taken together, these results demonstrate that PPE, a strong inducer of progressive emphysema *in vivo*, can induce apoptosis of ATII-like cells *in vitro* and for the first time we show that L-carnitine can provide protection against PPE-induced apoptosis of ATII cells. Furthermore, we confirmed an antioxidant role for L-carnitine in protecting ATII cells against H<sub>2</sub>O<sub>2</sub>-induced apoptosis.

# L-Carnitine attenuates emphysema development

Our metabolomics screen identified L-carnitine to be one of the most significantly reduced metabolites in the lung during the progression of PPE-induced emphysema. This, along with its protective function against PPE-induced apoptosis of LA4 cells described above, prompted us to examine whether supplementation of mice with L-carnitine could attenuate the development of PPE-induced emphysema. Mice were supplemented every second day i.p. with L-carnitine at a dose of 500 mg/kg of body weight [28,45] following a single oropharyngeal administration of PPE. Figure 6(A) highlights that systemic application of L-carnitine results in a significant increase in the concentration of lungspecific L-carnitine at day 28 compared with animals only administered PPE and that this was approaching levels detected in PBS-treated control mice. Differential cell counts of cytospins obtained from the BALF confirmed that, by day 28, emphysema was progressing independently of inflammation in PPE-treated mice (Figure 6B). Interestingly, Western blot analysis of lung

homogenate revealed increased levels of active cleaved caspase 3, the executioner of apoptosis [46], in mice treated with PPE compared with control PBS and that this was reduced following supplementation with L-carnitine (Figure 6C). Furthermore, morphological analysis of tissue sections stained for cleaved caspase 3 demonstrated the presence of apoptotic alveolar epithelial cells, airway epithelial cells and endothelial cells within the lung of emphysematous mice induced by PPE (Figure 6D). The presence of apoptotic alveolar epithelial cells was drastically reduced following L-carnitine supplementation, as confirmed by quantification using the newCAST system (P < 0.01; Figure 6D), but some apoptotic endothelial and airway epithelial cells could still be detected in the supplemented group albeit to a lesser extent than in mice treated with PPE only.

Finally, we analysed physiological and pathological parameters in the above emphysematous mice. We observed an improved lung function following L-carnitine supplementation (Figure 7A). PPE-treated animals had increased lung compliance  $(0.067 \pm 0.008 \text{ ml/cmH}_2\text{O})$  compared with  $0.035 \pm 0.005 \text{ ml/cmH}_2\text{O}$ , P < 0.0001) compared with PBStreated controls, which improved following supplementation with L-carnitine  $0.051 \pm 0.006$  ml/cmH<sub>2</sub>O, P < 0.01 compared with mice treated with only PPE. This was accompanied by a concomitant increase (P < 0.05) in lung elastance of L-carnitine supplemented PPE-treated mice compared with their PPE-treated counterparts (Figure 7A). Furthermore, the increase in TLC observed in PPE-treated mice compared with PBS-treated controls  $(0.93 \pm 0.11 \text{ compared with } 0.63 \pm 0.08, P < 0.001)$ , was slightly reduced following L-carnitine supplementation (0.81  $\pm$  0.07) but did not reach statistical significance when compared with PPEtreated mice (Figure 7A). Surprisingly, despite a clear demonstration of enlargement of the airspaces in H&E-stained lung sections from PPE-treated mice compared with control animals, consistent

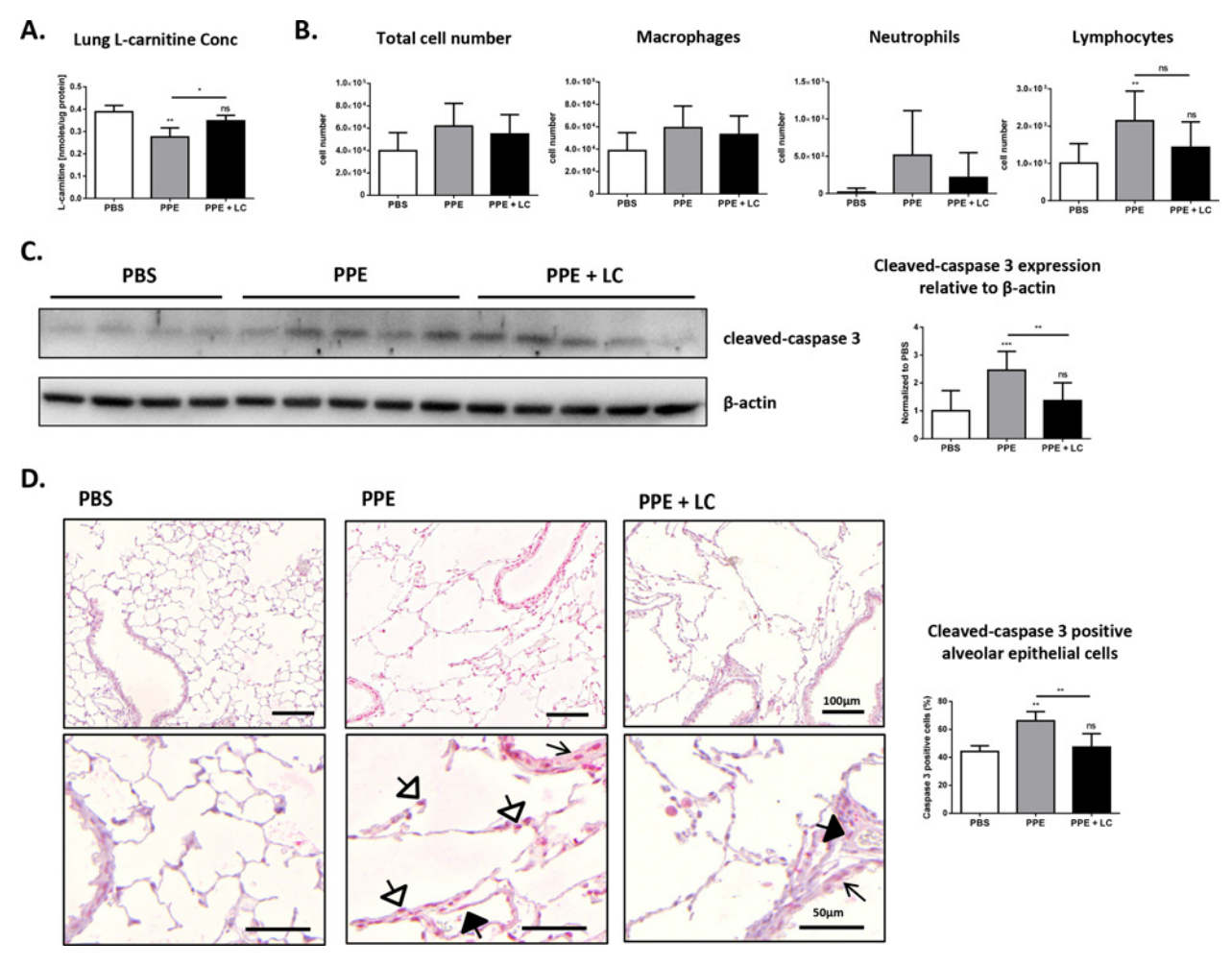


Figure 6 Supplementing mice with L-carnitine replenishes lung L-carnitine levels and is accompanied by an improvement in apoptosis levels

Mice were supplemented every second day i.p. with L-carnitine (LC) at a dose of 500 mg/kg of body weight following a single oropharyngeal administration of PPE. Mice were analysed 28 days later compared with mice that only received PPE or PBS controls. The experiment was repeated twice with n=4-6 mice per group each time. (A) The concentration of lung-specific free L-carnitine normalized to protein levels at 28 days. (B) Total and differential cell counts in the BALF. (C) Representative western blot and densitometric analysis for cleaved (active)-caspase 3 in lung homogenate of the mice indicated. (D). Representative photomicrographs of immunohistochemically stained lung sections with anti-cleaved caspase 3 antibody. Positively stained cells in red: open arrowhead indicates alveolar epithelial cell, closed arrowhead indicates endothelial cell, full arrow indicates airway epithelial cell. Scale bars: upper images =  $100~\mu\text{m}$ ; lower images =  $50~\mu\text{m}$ . Quantification of cleaved caspase 3-positive alveolar epithelial cells using the newCAST system was calculated. Data shown in all charts are the mean values  $\pm$  S.D., with \*P < 0.05, \*\*P < 0.01, \*\*\*P < 0.001; ns, not significant, one-way ANOVA followed by Bonferroni's post-hoc test.

with their poor lung function, we did not observe an improved airspace enlargement to accompany the improved lung function observed in the L-carnitine supplemented mice (Figure 7B). Taken together, L-carnitine supplementation protects against the alveolar cell apoptosis that accompanies emphysema progression and improves lung function in PPE-induced emphysematous mice.

# **DISCUSSION**

The present study used MS-based targeted metabolomics followed by systems biological approaches to quantify the lung tissue, BALF and serum metabolome at three different time points during emphysema progression in the PPE-induced murine model, to further elucidate mechanisms of progression in emphysema development. We demonstrate that changes in the metabolome are compartment-specific, with a greater change being detected local to the lung rather than the serum and for the first time reported that emphysema progression is accompanied by a reduction in lung-specific L-carnitine. Furthermore, supplementation with L-carnitine impaired apoptosis of alveolar cells both *in vitro* and *in vivo* and this was accompanied by an improvement in lung function of PPE-induced emphysematous mice.

Metabolomics is a powerful tool that can reveal a greater depth of understanding about the biochemical pathways of cells, thus

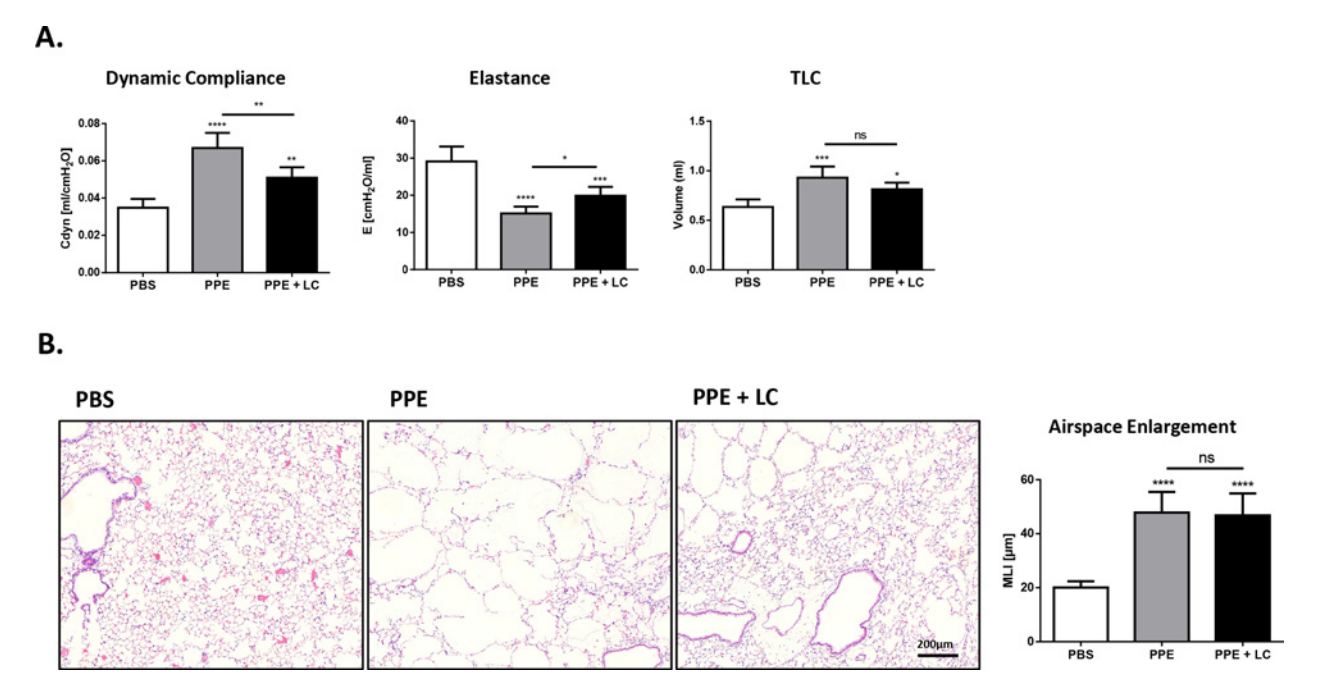


Figure 7 L-Carnitine supplementation improves lung function in PPE-induced emphysematous mice
(A) Lung function measurements to obtain dynamic compliance, elastance and TLC were carried out on day 28 in PBS-, PPE- and PPE-treated mice supplemented with L-carnitine (LC) every second day at 500 mg/kg of body weight i.p. (B) Representative photomicrographs of H&E-stained lung sections from the three groups of mice. Scale bar = 200 μm. Airspace enlargement was quantified as the MLI by design-based stereology of the H&E-stained lung sections using the newCAST system. All data shown are the mean values ± S.D. from two experiments, n = 4-6 per group, one-way ANOVA followed by Bonferroni's post-hoc test with \*P < 0.05, \*\*P < 0.01, \*\*\*P < 0.001, \*\*\*\*P < 0.0001; ns, not significant.</p>

providing a detailed profiling of the physiological changes in tissues and organisms during steady state and disease progression, than simply gene expression, to potentially reveal new underlying pathophysiological mechanisms and biomarkers of disease progression. This is substantiated by the rapid increase in studies over the last 5 years assessing metabolomic changes in COPD patients and animal models of disease [10-17]. These studies, however, lack a thorough analysis of metabolomic changes occurring in the lung tissue during the progression of emphysema. This may not be the ideal tissue for a biomarker given the difficulties in obtaining biopsies from patients, but it is critical in furthering our understanding of the mechanisms of disease progression. To that end we chose to assess the well-established PPE-induced murine model of emphysema, as it induces airspace enlargement similar to that observed in COPD patients [36], a single treatment leads to progressive disease that is associated with senescence of alveolar epithelial cells [19] and accompanied by increased levels of apoptosis [47]. In the present study, we confirm that a single oropharyngeal application of PPE resulted in a progressive emphysematous phenotype to day 161, which is associated with a steady decline in lung function and an increase in lung volume that accompanies an increase in airspace enlargement. We also demonstrate that PPE-induced emphysema is accompanied by increased levels of apoptosis in alveolar epithelial cells, airway epithelial cells and endothelial cells.

Pulmonary surfactant secreted by alveolar epithelial type II cells to reduce pulmonary surface tension at the air/liquid inter-

face of alveolar spaces is composed of key surfactant proteins and several classes of lipid, with 80% of surfactant lipid consisting of PC [48]. Ridsdale et al. [38] demonstrated that the BALF of emphysematous patients contained less PC C<sub>16:0</sub>/C<sub>14:0</sub> compared with controls and a study examining airway epithelial cells isolated from mice exposed to cigarette smoke for 8 weeks reported a decrease of 61 % in the level of total PC compared with filtered air controls [39]. Our analysis of altered metabolites clearly demonstrates, from day 56 onwards, a significant reduction in PC family members in both the lung tissue sample and the BALF. Indeed, over 40 PC family members of both diacylPC and acyl-alkylPC species were significantly reduced in the BALF at days 56 and 161, including PC C<sub>30:0</sub>, the same lipid as described in the patient study. Two other major PC components of pulmonary surfactant PC  $C_{16:0}/C_{16:0}$  and PC  $C_{16:0}/C_{16:1}$  [49] were also significantly reduced in the BALF of PPE-exposed mice at days 56 and 161 compared with PBS controls. It is interesting to highlight that L-carnitine has been reported to be important for the production of pulmonary surfactant PC in the fetal lung. Treatment of pregnant rats with L-carnitine resulted in significant increases in the amounts of both total phospholipid and PC C<sub>16:0</sub>/C<sub>16:0</sub> in fetal rat lung, which was accompanied by increased numbers of lamellar bodies in alveolar epithelial type II cell progenitors [50]. Our metabolic screen revealed significant reduction in the levels of lung L-carnitine, including free L-carnitine ( $C_0$ ) and L-carnitine C<sub>16</sub> (L-carnitine is attached to the same length fatty acid chain that is found attached to the predominant PCs of pulmonary surfactant) from day 56 onwards, which coincides with the reduction in BALF PC. One could therefore speculate that the reduction observed in PC is the result of lowered levels of L-carnitine in the emphysematous lung during disease progression.

We also demonstrated that the emphysematous lung and BALF compared with control mice contained reduced levels of SM lipids with both long-chain and very-long-chain fatty acids attached. A very recent study of COPD patients, using both targeted and untargeted metabolic approaches, revealed an inverse association between the level of some plasma SM and emphysema severity [15]. Of the five SM validated by both screens in that study, four were also reduced in our study and the fifth SM C<sub>14:0</sub> was not detected by our kit. We did not detect any significant changes in the levels of serum SM in contrast with the patient study. However, another group assessing the level of plasma SM in 3840 participants and measuring pulmonary emphysema using computed tomography reported higher plasma levels of SM was associated with increased progression of emphysema [51].

Our most interesting observation is that the progression of emphysema is associated with a reduction in the levels of lung L-carnitine; in fact, by day 161, L-carnitine had become the most significantly altered metabolite in the lung. Interestingly, Elsammak et al. [52] previously demonstrated a significant reduction in plasma total and free carnitine levels in COPD patients compared with healthy controls, which significantly correlated with severe (FEV1  $\geq$  30% to <50% predicted) and very severe (FEV1 <30%) patients only [52]. The primary function of L-carnitine is to transport long-chain fatty acids into the mitochondrial matrix for their subsequent  $\beta$ -oxidation and energy production via the tricarboxylic acid cycle [20]. Long-chain fatty acids are first activated by the enzyme long-chain acyl-CoA synthetase in the mitochondrial outer membrane to form acyl-CoAs, which cannot enter the mitochondrial matrix. They are therefore catalysed by another mitochondrial outer membrane enzyme, carnitine palmitoyltransferase I, which replaces CoA with L-carnitine, to form the long-chain acylcarnitines. These are then transported into the mitochondrial matrix via the integral mitochondrial inner membrane protein carnitine:acylcarnitine translocase (CACT). The importance of L-carnitine is highlighted by newborns that suffer primary systemic carnitine deficiency due to mutations in the gene encoding OCTN2 [53], because of reduced  $\beta$ -oxidation energy production is down which particularly affects skeletal and cardiac muscles presenting as myopathy; if left unchecked, it can progress to a systemic syndrome of hypotonia, hypoglycaemia, hypoketonia, encephalopathy, coma and perhaps death; however, patients respond very well to L-carnitine supplementation [30]. In addition to its role in the oxidation of fatty acids, L-carnitine's ability to accept fatty acid chains from acyl-CoA means that it is important in regulating the ratio of free CoA to acyl-CoA. A reduction in the levels of L-carnitine results in a reduction in mitochondrial free CoA and increased acyl-CoA which inhibits the function of several mitochondrial dehydrogenases impairing carbohydrate utilization, amino acid catabolism and the detoxification of xenobiotics [54]. A lung with such disrupted metabolic homoeostasis is unlikely to have a balance in favour of repair and regeneration over injury.

In contrast with the deleterious effects of reduced L-carnitine, we have shown in the present study that apoptosis induced in the ATII-like cell line LA4 by both PPE and H<sub>2</sub>O<sub>2</sub> can be prevented by pre-treating the cells with L-carnitine. It has been suggested that PPE-treated lung epithelial cells up-regulate placental growth factor which induces apoptosis via signalling through the c-Jun N-terminal kinase (JNK) and p38 mitogen-activated protein kinase (MAPK) pathways [47]. Signalling through these kinases can result in the mitochondria-mediated (intrinsic) apoptotic pathway: translocation of Bax and Bim to the mitochondria, followed by cytochrome c release and caspase activation [55,56]. Mitochondrial permeability transition is a key for cytochrome crelease [57], and it is interesting to note that L-carnitine has been shown to inhibit the mitochondrial permeability transition on isolated rat liver mitochondria [58]. Furthermore, it has been demonstrated in vitro that L-carnitine has the ability to directly inhibit the proteolytic activity of both an initiator and an effector caspase, caspases 8 and 3 respectively [25]. Conventionally, one thinks of H<sub>2</sub>O<sub>2</sub>-induced apoptosis to progress through a mechanism of increased intracellular oxidants, mitochondrial membrane polarization, cytochrome c release and caspase activation, as has been described for alveolar epithelial type II cells [42]. We demonstrate that pre-treatment of LA4 cells with L-carnitine reduces the amount of mitochondrial superoxide production following H<sub>2</sub>O<sub>2</sub> treatment, which may offer another potential anti-apoptotic mode of action for L-carnitine, as has also been suggested following H<sub>2</sub>O<sub>2</sub> treatment of the human proximal tubule epithelial cell line HK-2 [21]. More intriguing is the mechanism of action demonstrated in cardiac myocytes that L-carnitine can block the increase in intracellular ceramide levels by inhibiting the action of acid sphingomyelinase [22]. Interestingly, up-regulation of ceramide has been shown to precede caspase 3 activation during apoptosis of A549 cells [59], although the increases in ceramide following H<sub>2</sub>O<sub>2</sub> treatment of human airway epithelial cells are via the action of neutral sphingomyelinase [43]. Increases in the levels of ceramide have also been associated with pulmonary cell apoptosis in animal models of emphysema and, in the same study, increased ceramide was also observed in the alveolar septal cells of emphysematous patients [44].

The benefit to mitochondrial homoeostasis described following L-carnitine supplementation and the positive effects on inhibiting apoptosis in vitro led us to hypothesize that supplementing with L-carnitine would attenuate the development of emphysema in PPE-treated mice. Supplementing mice i.p. with L-carnitine increased the level of lung L-carnitine following PPE treatment which was accompanied by a significant improvement in lung function and in the level of apoptosis. The caveat to this is that there did not appear to be any improvement to the airspace enlargement compared with PPE treatment alone. One potential reason for this and a critique of the study was the time of analysis following supplementation. We assessed the lungs 28 days post-instillation to examine whether L-carnitine supplementation early could slow the progression of emphysema; however, it is possible that L-carnitine is more important for disease progression rather than initiation. Additionally, the route of delivery for L-carnitine can also be discussed in this context. The lung as an organ manifests perfectly for local drug delivery, but we used i.p.

application. Aside from ease of administration, an in vivo study in mice using the ovalbumin model of asthma reported that i.p. delivery of L-carnitine improved oxygen saturation and improved bronchus-associated inflammation [28]; additionally, administration of L-carnitine in the drinking water of rats reduced the level of lipid peroxide found in the lung following bleomycin treatment [45]. In the present study, following i.p. administration of L-carnitine, L-carnitine levels in the lung were greater than PPEtreated mice alone, which was accompanied by an improvement in lung function and apoptosis. Immunohistochemistry of lung sections for activated caspase 3 revealed that apoptotic alveolar epithelial type II cells were reduced following L-carnitine supplementation, but some apoptotic endothelial and airway epithelial cells could still be detected in the supplemented group. The remaining apoptotic cells in the lungs of our supplemented mice may thus be preventing a balance in favour of regeneration and therefore comparable airspace enlargement is observed across the two groups. Sufficient blocking of apoptosis by inhibiting the MAPK pathways or using siRNA knockdown of placental growth factor-inhibited airspace enlargement following PPE exposure [47].

To expand upon the findings of the present study, we further plan to assess the beneficial effects of L-carnitine supplementation during chronic cigarette smoke exposure, a model of COPD in which emphysema is accompanied by chronic inflammation and airway remodelling [32,60]. It has been known for some time that oxidative stress following cigarette smoking is involved in many of the pathological processes underlying COPD [61] and, more recently, cigarette smoke has been shown to impair mitochondrial function [62]. L-Carnitine's established role as an antioxidant and enhancer of mitochondrial function [21,23,24] would thus lend it to having additional beneficial effects against chronic cigarette smoke-induced lung injury.

In summary, targeted metabolomics reveals for the first time that the progression of emphysema is accompanied by a reduction in the lungs of the metabolite L-carnitine. L-Carnitine supplementation impaired apoptosis of alveolar cells both *in vitro* and *in vivo* and this was accompanied by an improvement in lung function of PPE-induced emphysematous mice. We therefore suggest that L-carnitine supplementation of COPD patients in parallel with their current treatment regime could slow, or even regress, disease progression.

# **CLINICAL PERSPECTIVES**

- It is not clear what drives disease progression in emphysematous patients; indeed, progression among individuals is highly variable. Therefore, we performed a targeted metabolomics approach to identify novel metabolic pathways in a clinically relevant progressive emphysema mouse model, to highlight new targets and biomarkers that may be the key in furthering our understanding of disease progression.
- We demonstrate that changes to the metabolome were very compartmentalized with greater changes detectable in the lung tissue and BALF rather than the serum. Furthermore,

- the present study shows for the first time that emphysema progression is associated with a reduction in lung tissue-specific L-carnitine, a critical metabolite with antioxidant and antiapoptotic properties. Additionally, supplementing mice with this metabolite impeded disease progression.
- The identification of metabolomic changes local to the injured tissue are key in identifying good biomarkers for disease progression and critical in furthering our understanding of the mechanisms of disease progression and for identifying novel therapeutic targets.

#### **AUTHOR CONTRIBUTION**

Thomas Conlon, Korbinian Ballweg, Cornelia Prehn, Jerzy Adamski, Oliver Eickelberg and Ali Yildirim designed experiments. Thomas Conlon, Korbinian Ballweg and Cornelia Prehn conducted experiments. Jörg Bartel, Jan Krumsiek and Fabian Theis designed and undertook analysis of metabolomics data. Thomas Conlon and Ali Yildirim wrote the manuscript. All authors contributed to scientific discussions and read the manuscript.

#### **ACKNOWLEDGEMENTS**

We acknowledge the help of Christine Hollauer and Joanna Schmucker. We thank Julia Scarpa, Werner Römisch-Margl and Katharina Faschinger for metabolomics measurements performed at the Helmholtz Zentrum München, Genome Analysis Center, Metabolomics Core Facility.

#### FUNDING

This work was supported by the Helmholtz Association; the German Center for Lung Research (DZL); and the German Federal Ministry of Education and Research to the German Center for Diabetes Research (DZD e.V.).

# **REFERENCES**

- Pauwels, R.A., Buist, A.S., Calverley, P.M., Jenkins, C.R. and Hurd, S.S. (2001) Global strategy for the diagnosis, management, and prevention of chronic obstructive pulmonary disease. NHLBI/WHO Global Initiative for Chronic Obstructive Lung Disease (GOLD) Workshop summary. Am. J. Respir. Crit. Care Med. 163, 1256–1276 CrossRef PubMed
- McDonough, J.E., Yuan, R., Suzuki, M., Seyednejad, N., Elliott, W.M., Sanchez, P.G., Wright, A.C., Gefter, W.B., Litzky, L., Coxson, H.O. et al. (2011) Small-airway obstruction and emphysema in chronic obstructive pulmonary disease. N. Engl. J. Med. 365, 1567–1575 CrossRef PubMed
- 3 Hautamaki, R.D., Kobayashi, D.K., Senior, R.M. and Shapiro, S.D. (1997) Requirement for macrophage elastase for cigarette smoke-induced emphysema in mice. Science 277, 2002–2004 <u>CrossRef PubMed</u>
- Wiedemann, H.P. and Stoller, J.K. (1996) Lung disease due to alpha 1-antitrypsin deficiency. Curr. Opin. Pulm. Med. 2, 155–160 CrossRef PubMed
- 5 Kanazawa, H. and Yoshikawa, J. (2005) Elevated oxidative stress and reciprocal reduction of vascular endothelial growth factor levels with severity of COPD. Chest 128, 3191–3197 CrossRef PubMed

- 6 Tsuji, T., Aoshiba, K. and Nagai, A. (2006) Alveolar cell senescence in patients with pulmonary emphysema. Am. J. Respir. Crit. Care Med. 174, 886–893 CrossRef PubMed
- 7 Kasahara, Y., Tuder, R.M., Cool, C.D., Lynch, D.A., Flores, S.C. and Voelkel, N.F. (2001) Endothelial cell death and decreased expression of vascular endothelial growth factor and vascular endothelial growth factor receptor 2 in emphysema. Am. J. Respir. Crit. Care Med. 163, 737–744 CrossRef PubMed
- 8 Calabrese, F., Giacometti, C., Beghe, B., Rea, F., Loy, M., Zuin, R., Marulli, G., Baraldo, S., Saetta, M. and Valente, M. (2005) Marked alveolar apoptosis/proliferation imbalance in end-stage emphysema. Respir. Res. 6, 14 CrossRef PubMed
- 9 Mittelstrass, K., Ried, J.S., Yu, Z., Krumsiek, J., Gieger, C., Prehn, C., Roemisch-Margl, W., Polonikov, A., Peters, A., Theis, F.J. et al. (2011) Discovery of sexual dimorphisms in metabolic and genetic biomarkers. PLoS Genet. 7, e1002215 CrossRef PubMed
- Deja, S., Porebska, I., Kowal, A., Zabek, A., Barg, W., Pawelczyk, K., Stanimirova, I., Daszykowski, M., Korzeniewska, A., Jankowska, R. et al. (2014) Metabolomics provide new insights on lung cancer staging and discrimination from chronic obstructive pulmonary disease. J. Pharm. Biomed. Anal. 100, 369–380 CrossRef PubMed
- 11 Wang, L., Tang, Y., Liu, S., Mao, S., Ling, Y., Liu, D., He, X. and Wang, X. (2013) Metabonomic profiling of serum and urine by (1)H NMR-based spectroscopy discriminates patients with chronic obstructive pulmonary disease and healthy individuals. PLoS One 8, e65675 CrossRef PubMed
- Paige, M., Burdick, M.D., Kim, S., Xu, J., Lee, J.K. and Shim, Y.M. (2011) Pilot analysis of the plasma metabolite profiles associated with emphysematous chronic obstructive pulmonary disease phenotype. Biochem. Biophys. Res. Commun. 413, 588–593 CrossRef PubMed
- 13 Telenga, E.D., Hoffmann, R.F., Ruben, t.K., Hoonhorst, S.J., Willemse, B.W., van Oosterhout, A.J., Heijink, I.H., van den Berge, M., Jorge, L., Sandra, P. et al. (2014) Untargeted lipidomic analysis in chronic obstructive pulmonary disease. Uncovering sphingolipids. Am. J. Respir. Crit. Care Med. 190, 155–164 CrossRef PubMed
- 14 Ubhi, B.K., Cheng, K.K., Dong, J., Janowitz, T., Jodrell, D., Tal-Singer, R., MacNee, W., Lomas, D.A., Riley, J.H., Griffin, J.L. et al. (2012) Targeted metabolomics identifies perturbations in amino acid metabolism that sub-classify patients with COPD. Mol. Biosyst. 8, 3125–3133 CrossRef PubMed
- Bowler, R.P., Jacobson, S., Cruickshank, C., Hughes, G.J., Siska, C., Ory, D.S., Petrache, I., Schaffer, J.E., Reisdorph, N. and Kechris, K. (2015) Plasma sphingolipids associated with chronic obstructive pulmonary disease phenotypes. Am. J. Respir. Crit. Care Med. 191, 275–284 CrossRef PubMed
- 16 Cruickshank-Quinn, C.I., Mahaffey, S., Justice, M.J., Hughes, G., Armstrong, M., Bowler, R.P., Reisdorph, R., Petrache, I. and Reisdorph, N. (2014) Transient and persistent metabolomic changes in plasma following chronic cigarette smoke exposure in a mouse model. PLoS One 9, e101855 CrossRef PubMed
- Li, J., Yang, L., Li, Y., Tian, Y., Li, S., Jiang, S., Wang, Y. and Li, X. (2015) Metabolomics study on model rats of chronic obstructive pulmonary disease treated with BuFei JianPi. Mol. Med. Rep. 11, 1324–1333 PubMed
- Yildirim, A.O., Muyal, V., John, G., Muller, B., Seifart, C., Kasper, M. and Fehrenbach, H. (2010) Palifermin induces alveolar maintenance programs in emphysematous mice. Am. J. Respir. Crit. Care Med. 181, 705–717 CrossRef PubMed
- 19 Sarker, R.S., John-Schuster, G., Bohla, A., Mutze, K., Burgstaller, G., Bedford, M.T., Konigshoff, M., Eickelberg, O. and Yildirim, A.Ö. (2015) Coactivator-associated arginine methyltransferase-1 function in alveolar epithelial senescence and elastase-induced emphysema susceptibility. Am. J. Respir. Cell Mol. Biol. 53, 769–781 PubMed

- 20 Kerner, J. and Hoppel, C. (2000) Fatty acid import into mitochondria. Biochim. Biophys. Acta 1486, 1–17 CrossRef PubMed
- 21 Ye, J., Li, J., Yu, Y., Wei, Q., Deng, W. and Yu, L. (2010) L-carnitine attenuates oxidant injury in HK-2 cells via ROS-mitochondria pathway. Regul. Pept. 161, 58–66 CrossRef PubMed
- 22 Andrieu-Abadie, N., Jaffrezou, J.P., Hatem, S., Laurent, G., Levade, T. and Mercadier, J.J. (1999) L-carnitine prevents doxorubicin-induced apoptosis of cardiac myocytes: role of inhibition of ceramide generation. FASEB J. 13, 1501–1510 PubMed
- 23 Calo, L.A., Pagnin, E., Davis, P.A., Semplicini, A., Nicolai, R., Calvani, M. and Pessina, A.C. (2006) Antioxidant effect of L-carnitine and its short chain esters: relevance for the protection from oxidative stress related cardiovascular damage. Int. J. Cardiol. 107, 54–60 CrossRef PubMed
- 24 Geier, D.A. and Geier, M.R. (2013) L-carnitine exposure and mitochondrial function in human neuronal cells. Neurochem. Res. 38, 2336–2341 CrossRef PubMed
- Mutomba, M.C., Yuan, H., Konyavko, M., Adachi, S., Yokoyama, C.B., Esser, V., McGarry, J.D., Babior, B.M. and Gottlieb, R.A. (2000) Regulation of the activity of caspases by L-carnitine and palmitoylcarnitine. FEBS Lett. 478, 19–25 CrossRef PubMed
- Vescovo, G., Ravara, B., Gobbo, V., Sandri, M., Angelini, A., Della Barbera, M., Dona, M., Peluso, G., Calvani, M., Mosconi, L. et al. (2002) L-Carnitine: a potential treatment for blocking apoptosis and preventing skeletal muscle myopathy in heart failure. Am. J. Physiol. Cell Physiol. 283, C802–C810 CrossRef PubMed
- 27 Al-Biltagi, M., Isa, M., Bediwy, A.S., Helaly, N. and El Lebedy, D.D. (2012) L-carnitine improves the asthma control in children with moderate persistent asthma. J. Allergy 2012, 509730 CrossRef PubMed
- Uzuner, N., Kavukcu, S., Yilmaz, O., Ozkal, S., Islekel, H., Karaman, O., Soylu, A. and Kargi, A. (2002) The role of L-carnitine in treatment of a murine model of asthma. Acta Med. Okayama 56, 295–301 PubMed
- 29 Borghi-Silva, A., Baldissera, V., Sampaio, L.M., Pires-DiLorenzo, V.A., Jamami, M., Demonte, A., Marchini, J.S. and Costa, D. (2006) L-carnitine as an ergogenic aid for patients with chronic obstructive pulmonary disease submitted to whole-body and respiratory muscle training programs. Braz. J. Med. Biol. Res. 39, 465–474 CrossRef PubMed
- 30 Crill, C.M. and Helms, R.A. (2007) The use of carnitine in pediatric nutrition. Nutr. Clin. Pract. 22, 204–213 CrossRef PubMed
- 31 John, G., Kohse, K., Orasche, J., Reda, A., Schnelle-Kreis, J., Zimmermann, R., Schmid, O., Eickelberg, O. and Yildirim, A.O. (2014) The composition of cigarette smoke determines inflammatory cell recruitment to the lung in COPD mouse models. Clin. Sci. 126, 207–221 CrossRef PubMed
- 32 John-Schuster, G., Hager, K., Conlon, T.M., Irmler, M., Beckers, J., Eickelberg, O. and Yildirim, A.O. (2014) Cigarette smoke-induced iBALT mediates macrophage activation in a B cell-dependent manner in COPD. Am. J. Physiol. Lung Cell. Mol. Physiol. 307, L692–L706 CrossRef PubMed
- 33 Romisch-Margl, W., Prehn, C., Bogumil, R., Rohring, C., Suhre, K. and Adamski, J. (2012) Procedure for tissue sample preparation and metabolite extraction for high-throughput targeted metabolomics. Metabolomics 8, 133–142 CrossRef
- 34 Zukunft, S., Sorgenfrei, M., Prehn, C., Moller, G. and Adamski, J. (2013) Targeted metabolomics of dried blood spot extracts. Chromatographia 76, 1295–1305 <u>CrossRef</u>
- 35 Li, H.D., Xu, Q.S. and Liang, Y.Z. (2014) libPLS: An integrated library for partial least squares regression and discriminant analysis. PeerJ. PrePrints **2**, e190v191
- 36 Lucey, E.C., Keane, J., Kuang, P.P., Snider, G.L. and Goldstein, R.H. (2002) Severity of elastase-induced emphysema is decreased in tumor necrosis factor-alpha and interleukin-1beta receptor-deficient mice. Lab. Invest. 82, 79–85 CrossRef PubMed

- 37 Stone, P.J., Lucey, E.C., Calore, J.D., McMahon, M.P., Snider, G.L. and Franzblau, C. (1988) Defenses of the hamster lung against human neutrophil and porcine pancreatic elastase. Respiration 54, 1–15 CrossRef PubMed
- 38 Ridsdale, R., Roth-Kleiner, M., D'Ovidio, F., Unger, S., Yi, M., Keshavjee, S., Tanswell, A.K. and Post, M. (2005) Surfactant palmitoylmyristoylphosphatidylcholine is a marker for alveolar size during disease. Am. J. Respir. Crit. Care Med. 172, 225–232 CrossRef PubMed
- 39 Agarwal, A.R., Yin, F. and Cadenas, E. (2014) Short-term cigarette smoke exposure leads to metabolic alterations in lung alveolar cells. Am. J. Respir. Cell Mol. Biol. 51, 284–293 PubMed
- 40 Lorber, A., Wangen, L.E. and Kowalski, B.R. (1987) A theoretical foundation for the PLS algorithm. J. Chemom. 1, 19–31 CrossRef
- 41 Yano, T., Itoh, Y., Yamada, M., Egashira, N. and Oishi, R. (2008)
  Combined treatment with L-carnitine and a pan-caspase inhibitor
  effectively reverses amiodarone-induced injury in cultured human
  lung epithelial cells. Apoptosis 13, 543–552 CrossRef PubMed
- 42 Yin, L., Stearns, R. and Gonzalez-Flecha, B. (2005) Lysosomal and mitochondrial pathways in H<sub>2</sub>O<sub>2</sub>-induced apoptosis of alveolar type II cells. J. Cell. Biochem. 94, 433–445 CrossRef PubMed
- 43 Castillo, S.S., Levy, M., Thaikoottathil, J.V. and Goldkorn, T. (2007) Reactive nitrogen and oxygen species activate different sphingomyelinases to induce apoptosis in airway epithelial cells. Exp. Cell Res. 313, 2680–2686 CrossRef PubMed
- 44 Petrache, I., Natarajan, V., Zhen, L., Medler, T.R., Richter, A.T., Cho, C., Hubbard, W.C., Berdyshev, E.V. and Tuder, R.M. (2005) Ceramide upregulation causes pulmonary cell apoptosis and emphysema-like disease in mice. Nat. Med. 11, 491–498 CrossRef PubMed
- 45 Daba, M.H., Abdel-Aziz, A.A., Moustafa, A.M., Al-Majed, A.A., Al-Shabanah, O.A. and El-Kashef, H.A. (2002) Effects of L-carnitine and ginkgo biloba extract (EG b 761) in experimental bleomycin-induced lung fibrosis. Pharmacol. Res. 45, 461–467 CrossRef PubMed
- 46 Budihardjo, I., Oliver, H., Lutter, M., Luo, X. and Wang, X. (1999) Biochemical pathways of caspase activation during apoptosis. Annu. Rev. Cell. Dev. Biol. 15, 269–290 CrossRef PubMed
- 47 Hou, H.H., Cheng, S.L., Liu, H.T., Yang, F.Z., Wang, H.C. and Yu, C.J. (2013) Elastase induced lung epithelial cell apoptosis and emphysema through placenta growth factor. Cell Death Dis. 4, e793 CrossRef PubMed
- 48 Agassandian, M. and Mallampalli, R.K. (2013) Surfactant phospholipid metabolism. Biochim. Biophys. Acta 1831, 612–625 CrossRef PubMed
- 49 Bernhard, W., Hoffmann, S., Dombrowsky, H., Rau, G.A., Kamlage, A., Kappler, M., Haitsma, J.J., Freihorst, J., von der Hardt, H. and Poets, C.F. (2001) Phosphatidylcholine molecular species in lung surfactant: composition in relation to respiratory rate and lung development. Am. J. Respir. Cell Mol. Biol. 25, 725–731 CrossRef PubMed
- 50 Lohninger, A., Bock, P., Dadak, C., Feiks, A. and Kaiser, E. (1990) Effect of carnitine on foetal rat lung dipalmitoyl phosphatidylcholine content and lung morphology. Carnitine and lung surfactant, I. J. Clin. Chem. Clin. Biochem. 28, 313–318 PubMed

- 51 Ahmed, F.S., Jiang, X.C., Schwartz, J.E., Hoffman, E.A., Yeboah, J., Shea, S., Burkart, K.M. and Barr, R.G. (2014) Plasma sphingomyelin and longitudinal change in percent emphysema on CT. The MESA lung study. Biomarkers 19, 207–213 PubMed
- 52 Elsammak, M. M. Y., Attia, A. and Suleman, M. (2011) Carnitine deficiency in chronic obstructive pulmonary disease patients. J. Pulmonar. Respirat. Med. 1, 106 CrossRef
- Nezu, J., Tamai, I., Oku, A., Ohashi, R., Yabuuchi, H., Hashimoto, N., Nikaido, H., Sai, Y., Koizumi, A., Shoji, Y. et al. (1999) Primary systemic carnitine deficiency is caused by mutations in a gene encoding sodium ion-dependent carnitine transporter. Nat. Genet. 21, 91–94
  CrossRef PubMed
- Marcovina, S.M., Sirtori, C., Peracino, A., Gheorghiade, M., Borum, P., Remuzzi, G. and Ardehali, H. (2013) Translating the basic knowledge of mitochondrial functions to metabolic therapy: role of L-carnitine. Transl. Res. 161, 73–84 CrossRef PubMed
- Kurinna, S.M., Tsao, C.C., Nica, A.F., Jiffar, T. and Ruvolo, P.P. (2004) Ceramide promotes apoptosis in lung cancer-derived A549 cells by a mechanism involving c-Jun NH2-terminal kinase. Cancer Res. 64, 7852–7856
  CrossRef PubMed
- Van Laethem, A., Van Kelst, S., Lippens, S., Declercq, W., Vandenabeele, P., Janssens, S., Vandenheede, J.R., Garmyn, M. and Agostinis, P. (2004) Activation of p38 MAPK is required for Bax translocation to mitochondria, cytochrome c release and apoptosis induced by UVB irradiation in human keratinocytes. FASEB J. 18, 1946–1948 PubMed
- Narita, M., Shimizu, S., Ito, T., Chittenden, T., Lutz, R.J., Matsuda, H. and Tsujimoto, Y. (1998) Bax interacts with the permeability transition pore to induce permeability transition and cytochrome c release in isolated mitochondria. Proc. Natl. Acad. Sci. U.S.A. 95, 14681–14686 CrossRef PubMed
- 58 Pastorino, J.G., Snyder, J.W., Serroni, A., Hoek, J.B. and Farber, J.L. (1993) Cyclosporin and carnitine prevent the anoxic death of cultured hepatocytes by inhibiting the mitochondrial permeability transition. J. Biol. Chem. 268, 13791–13798 PubMed
- Ravid, T., Tsaba, A., Gee, P., Rasooly, R., Medina, E.A. and Goldkorn, T. (2003) Ceramide accumulation precedes caspase-3 activation during apoptosis of A549 human lung adenocarcinoma cells. Am. J. Physiol. Lung Cell. Mol. Physiol. 284, L1082–L1092 CrossRef PubMed
- John-Schuster, G., Günter, S., Hager, K., Conlon, T.M., Eickelberg, O. and Yildirim, A.Ö. (2015) Inflammaging increases susceptibility to cigarette smoke-induced COPD. Oncotarget. 4027 PubMed
- 61 MacNee, W. (2005) Oxidants and COPD. Curr. Drug Targets Inflamm. Allergy 4, 627–641 CrossRef PubMed
- 62 Ballweg, K., Mutze, K., Konigshoff, M., Eickelberg, O. and Meiners, S. (2014) Cigarette smoke extract affects mitochondrial function in alveolar epithelial cells. Am. J. Physiol. Lung Cell. Mol. Physiol. 307, L895–L907 CrossRef PubMed

Received 19 June 2015/6 November 2015; accepted 12 November 2015 Accepted Manuscript online 12 November 2015, doi: 10.1042/CS20150438